

Minireview

The mechanism of the alkaline phosphatase reaction: insights from NMR, crystallography and site-specific mutagenesis

Kathleen M. Holtz, Evan R. Kantrowitz*

Department of Chemistry, Merkert Chemistry Center, Boston College, Chestnut Hill, MA 02467, USA

Received 23 August 1999

Abstract The proposed double in-line displacement mechanism of *Escherichia coli* alkaline phosphatase (AP) involving two-metal ion catalysis is based on NMR spectroscopic and X-ray crystallographic studies. This mechanism is further supported by the X-ray crystal structures of the covalent phospho-enzyme intermediate of the H331Q mutant AP and of the transition state complex between the wild-type enzyme and vanadate, a transition state analog. Kinetic and structural studies on several genetically engineered versions of AP illustrate the overall importance of the active site's metal geometry, hydrogen bonding network and electrostatic potential in the catalytic mechanism.

© 1999 Federation of European Biochemical Societies.

Key words: Mechanism; Phosphatase; Rate-limiting step; Site-specific mutagenesis; Transphosphorylation; Trigonal bipyramidal

1. Introduction

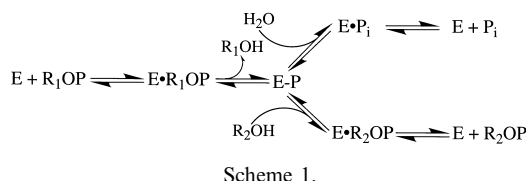
Alkaline phosphatase from *Escherichia coli* (AP, EC 3.1.3.1) is a homodimeric, non-specific phosphomonoesterase consisting of 449 amino acids per monomer. The overall molecule is approximately $100 \text{ \AA} \times 50 \text{ \AA} \times 50 \text{ \AA}$ with the two active sites approximately 30 \AA apart. The shallow active site pocket has no apparent binding site for the R group of the phosphate monoester consistent with the non-specificity of AP [1]. Each active site contains three closely spaced metal binding sites identified as A, B, and C in NMR studies and as M1, M2, and M3 in X-ray crystallographic studies. Zinc ions occupy the M1 and M2 sites and a magnesium ion occupies the M3 site. Catalysis requires M1 site occupancy and is greatly enhanced by M2 site occupancy [2,3]. The enzyme-catalyzed reaction has an alkaline pH maximum and is diffusion-controlled [4].

E. coli AP is a prototype for all alkaline phosphatases, especially the mammalian alkaline phosphatases. Sequence comparisons show only 25–30% sequence homology between the *E. coli* enzyme and the yeast and mammalian enzymes [5–8]. The active site regions of these alkaline phosphatases from different organisms are highly conserved with differences at only three positions [9,10]. Further, functionally related phosphoesterases including phospholipase C from *Bacillus cereus* [11] and P1 nuclease from *Penicillium citrinum* [12] have metal triads in their active sites similar to AP. The extensive investigations into the catalytic mechanism of the bacterial enzyme

stem from its ability to serve as a model for other alkaline phosphatases and other phosphatases that use metal ions in phosphate ester hydrolysis and transfer reactions.

2. Kinetic scheme of AP

In the accepted kinetic scheme for the enzymatic hydrolysis/transphosphorylation of phosphate monoesters by AP (Scheme 1) [13], the nucleophile, Ser-102, is transiently phosphorylated giving a covalent phosphoseryl intermediate (E-P) [14]. The covalent E-P intermediate is subsequently hydrolyzed to give a non-covalent enzyme-phosphate complex (E·P_i). In the presence of a phosphate acceptor such as Tris or ethanolamine, the enzyme exhibits transphosphorylation activity transferring phosphate to the alcohol to form another phosphate monoester [1,15,16]. Consistent with the double displacement mechanism and the formation of a covalent E-P intermediate, the overall reaction proceeds with retention of configuration [17].



3. Multinuclear NMR studies

The $E-P \rightleftharpoons E \cdot P_i$ equilibrium in Scheme 1 has been the subject of several NMR investigations [18–22]. ^{31}P NMR studies demonstrated that the hydrolysis of the covalent E-P intermediate is rate-limiting under acidic conditions, while the hydrolysis of the non-covalent $E \cdot P_i$ complex is rate-limiting under alkaline conditions [22]. Subsequent experiments using ^{31}P inversion transfer measured the rate of phosphate dissociation from the non-covalent $E \cdot P_i$ complex at alkaline pH ($\sim 30 \text{ s}^{-1}$) showing that this rate is approximately equal to the enzyme turnover rate (k_{cat}) [21]. The rate-limiting dissociation is essentially pH-independent between pH 6 and 9. Below pH 6, dephosphorylation becomes rate-limiting. The change in rate-limiting step from phosphate dissociation in the non-covalent $E \cdot P_i$ complex to dephosphorylation of the covalent E-P intermediate coincides with the sigmoidal pH versus activity profile and reflects the ionization state of a Zn-coordinated hydroxide nucleophile identified in other NMR studies. This Zn-coordinated hydroxide nucleophile controls the rate-limiting step in the mechanism.

*Corresponding author.

The Zn-coordinated nucleophile responsible for dephosphorylation of the covalent E-P intermediate was identified through ^{31}P NMR experiments [19]. The pH dependence of the $\text{E-P} \rightleftharpoons \text{E-P}_i$ equilibrium of the native enzyme ($\text{Zn}_4\text{Mg}_2\text{AP}$ or Zn_4AP)¹ gives a sigmoidal profile with a midpoint of pH 5. Cd substitution in the Cd_6AP and Cd_2AP enzymes² shifts the midpoint of this equilibrium by 4–5 units to a more alkaline pH [19,20]. The magnitude of this shift suggests that a metal-coordinated water molecule in the native enzyme controls the $\text{E-P} \rightleftharpoons \text{E-P}_i$ equilibrium and its pK_a is dependent on the hardness of the coordinating metal ion. Selective substitution of the B site metal ion with cadmium ($(\text{Zn}_A\text{Cd}_B)_2\text{AP}$)³ has a much less significant effect on the equilibrium midpoint compared to the Cd_6AP or Cd_2AP enzymes suggesting that the A site metal ion is responsible for coordinating the water molecule and lowering its pK_a [20]. This conclusion is supported by ^{113}Cd NMR studies of the Cd_6AP showing significant chemical shift perturbations in the Cd resonance corresponding to the A site metal in the presence of phosphate acceptors [21].

The precise relationship between the metal ions and phosphate could not be determined in detail from NMR studies. Considerable NMR evidence, however, supported a direct interaction between phosphate in the non-covalent E-P_i complex and the A site metal ion prompting a role for this ion in positioning substrates/phosphate for nucleophilic attack [19,20]. In contrast, the relative insensitivity of the E-P chemical shift with metal substitution at either the A or B sites led to the erroneous conclusion that the covalent E-P intermediate was not closely associated with the metal ions [19]. With the determination of the X-ray crystal structure, however, the bridging position of phosphate between both zinc ions in the A and B sites was observed and the specific roles of these ions in binding and catalysis could be assigned.

4. X-ray crystallography

The X-ray crystal structures of the non-covalent E-P_i complex in the native enzyme and the covalent E-P intermediate in the Cd-substituted enzyme are the basis for the proposed mechanism involving two-metal ion catalysis⁴ (Fig. 1) [23]. Based on the geometry of the metal binding sites, Zn_2 is positioned to coordinate the hydroxyl group of Ser-102 activating the O_γ oxygen atom for nucleophilic attack on the phosphorus atom of the substrate/phosphate. The position of Zn_1 is consistent with its dual role in coordinating the negatively charged leaving group of the substrate as an alkoxide ion in the first displacement step and then activating a solvent water molecule in the second step. The Zn_1 -coordi-

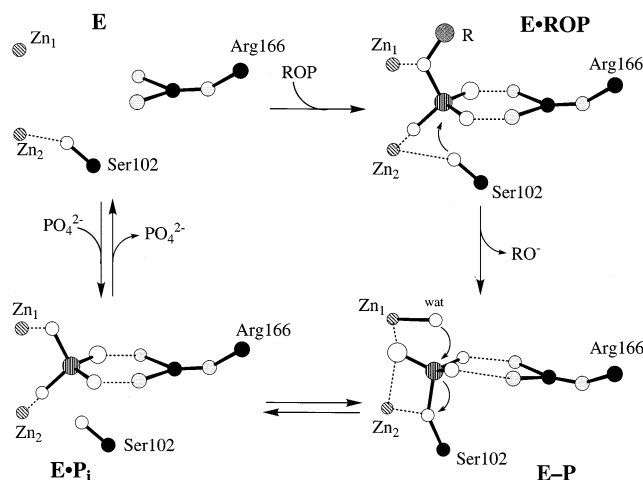


Fig. 1. Proposed mechanism of two-metal ion catalysis in the hydrolysis of phosphate monoesters by AP. Formation of the enzyme-substrate complex ($\text{E} \cdot \text{ROP}$) involves coordination of the ester oxygen to Zn_1 and additional interactions between the non-bridging oxygen atoms of the substrate, and Zn_2 and the guanidinium group of Arg-166. Ser-102 occupies the position opposite the leaving group. Upon formation of the covalent E-P intermediate, phosphate moves slightly into the active site cavity maintaining interactions to both Arg-166 and the zinc ions. At alkaline pH, a nucleophilic hydroxide coordinated to Zn_1 (identified as wat) attacks the covalent E-P intermediate forming the non-covalent E-P_i complex. The slow dissociation of phosphate from this complex is rate-limiting under alkaline conditions. The geometries of the E-P_i complex and the E-P intermediate come from the X-ray crystal structures of the native and Cd-substituted enzymes, respectively [23]. Hydrogen atoms, the magnesium ion, and the ligands to Zn_1 and Zn_2 are not shown.

nated water molecule which eluded detection in the X-ray structures of the native and Cd-substituted enzymes has been captured in the X-ray structure of the AP mutant H331Q [24]. In this structure, the Zn_1 -coordinated water molecule is optimally positioned for apical nucleophilic attack on the collapsed phosphorus center of the phosphoserine intermediate (Fig. 2, middle panel). Based on NMR and X-ray crystallography, the zinc ions have direct roles in catalysis.

The movement of phosphate into the active site and the trajectory of the nucleophilic water molecule inferred from the structures of the non-covalent E-P_i complex of the native enzyme and of the covalent E-P intermediate of the H331Q enzyme (Fig. 2, top and middle panels) are consistent with the postulated trigonal bipyramidal transition state of the two inline displacement steps. The proposed transition state is further supported by the X-ray crystal structure of the native enzyme with bound vanadate ($\text{AP} \cdot \text{VO}_3$) [25]. Vanadate ion binds in the active site with penta-coordinate geometry (Fig. 2, bottom panel) placing the nucleophiles in the catalytic reaction, Ser-102 and the Zn_1 -coordinated water molecule, in opposite axial positions separated by $\sim 170^\circ$. The covalent bond distances of the axial groups and the position of vanadate is clearly intermediate between those of the E-P_i complex and the phosphoserine intermediate. Three vanadium oxygen atoms spaced $\sim 120^\circ$ apart bisect the axial plane forming stabilizing interactions with Arg-166 and the zinc ions. In the conversion of the covalent E-P intermediate to the non-covalent E-P_i complex, Arg-166 remains in essentially the same position while the side chain of Ser-102 undergoes a small rotation (0.8 Å, Fig. 2). Only minor changes in the positions

¹ $\text{Zn}_4\text{Mg}_2\text{AP}$ refers to the native enzyme having two zinc ions and one magnesium in each active site. Zn_4AP refers to the enzyme containing a total of four zinc ions, two in the A and B sites of each active site.

² Cd_6AP refers to the Cd-substituted enzyme having all three metal binding sites in each active site replaced with cadmium ions. Cd_2AP refers to the Cd-substituted enzyme having only A site metal ions.

³ $(\text{Zn}_A\text{Cd}_B)_2\text{AP}$ refers to the mixed metal hybrid enzyme having a zinc ion in the A site and a cadmium ion in the B site of each active site.

⁴ Herein, Zn_1 , Zn_2 , and Mg correspond to the metal ion species in the M1, M2, and M3 binding sites, respectively. Zn_1 is Zn^{2+} bound in the M1 site; Zn_2 is Zn^{2+} bound in the M2 site; Mg is Mg^{2+} bound in the M3 site.

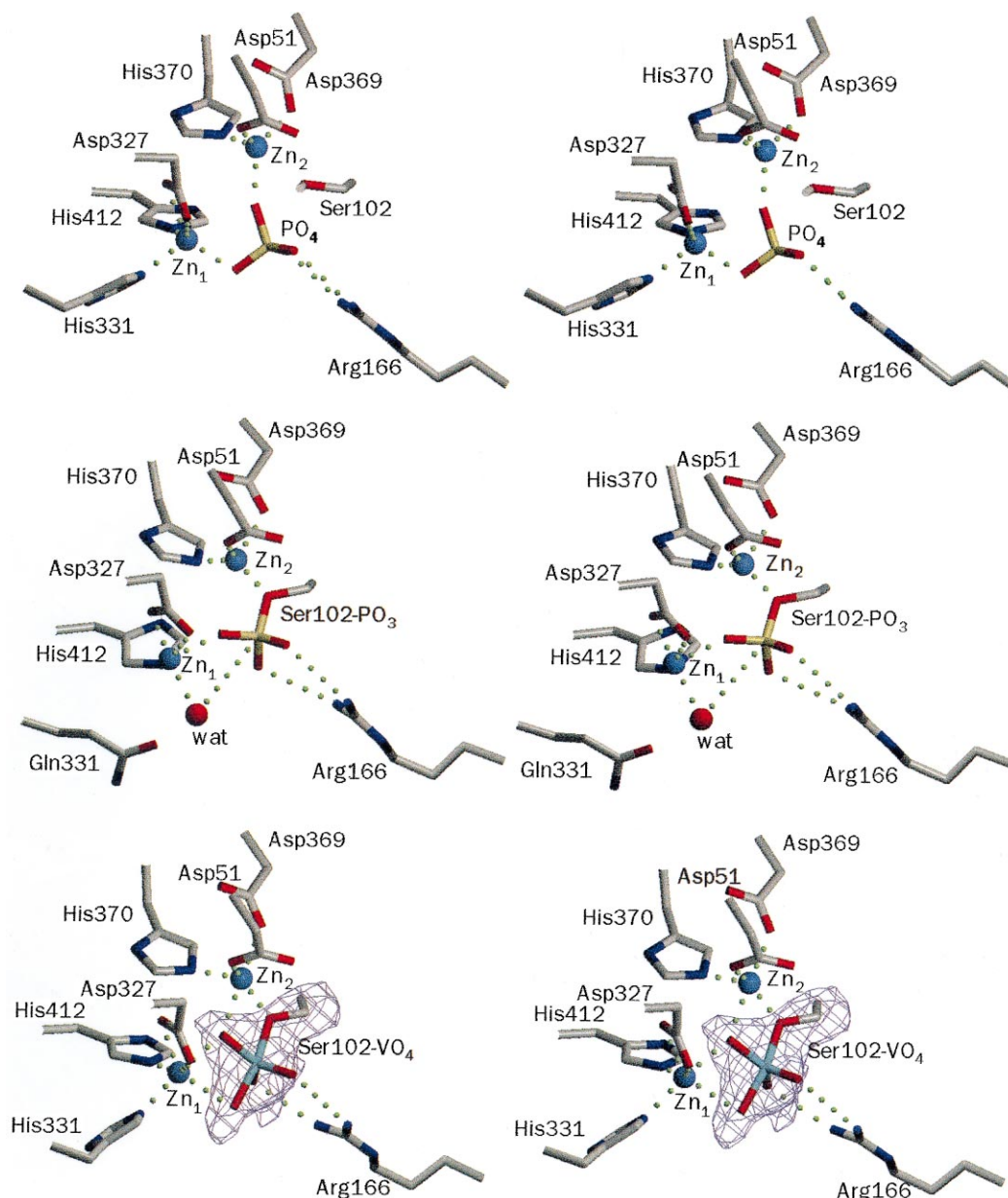


Fig. 2. (Top panel) Stereo view of the non-covalent E-P_i complex. Shown are Zn₁ and Zn₂ with side chain ligands, phosphate (labeled PO₄), Ser-102 nucleophile, and Arg-166. Coordinates for the wild-type enzyme with phosphate bound were taken from Protein Data Bank file 1ALK. (Middle panel) Stereo view of the covalent E-P intermediate. The covalent E-P intermediate (Ser-102-PO₃) is captured in the H331Q structure. The activated water molecule (red sphere labeled wat) is coordinated to Zn₁ (2.2 Å). Coordinates for the H331Q structure were taken from Protein Data Bank file 1HJK. (Bottom panel) Stereo view of vanadate bound in the active site of *E. coli* AP. The omit electron density map is drawn in stereo at a contour level of 3.0σ. The vanadate ion is bound to the nucleophilic serine residue (Ser-102-VO₄) in a position intermediate between those of the covalent E-P intermediate and the non-covalent E-P_i complex. The free axial oxygen atom of the vanadate ion is 2.4 Å from the Zn₁ site. Panels were drawn with the program SETOR [42]. This figure was reprinted from the original manuscript [25] with copyright permission.

of Arg-166 and Ser-102 are observed in the transition state structure suggesting the active site arrangement of AP is optimal for stabilization of a trigonal bipyramidal species, a finding further supported from site-specific mutagenesis.

5. Site-specific mutagenesis

5.1. Site-specific mutagenesis of the active site nucleophile, Ser-102, suggests that the zinc ions are the critical catalytic elements

While Ser-102 is an optimal nucleophile, it is not absolutely

required to achieve significant rate enhancements over the uncatalyzed reaction based on a series of site-specific mutations, S102C, S102A, S102G, S102L [26–28]. These mutant enzymes exhibit variable activities significantly less than the wild-type enzyme, but ~10⁵–10⁷-fold greater than the non-enzymatic reaction [26]. Typically, a 10³–10⁴-fold reduction in *k*_{cat} is observed for these mutant enzymes compared to the wild-type enzyme [26,27]. Only a 100-fold reduction in *k*_{cat} is reported for the S102C mutant enzyme reflecting the ability of the cysteine side chain to take over the role of nucleophile [27,28]. Although not positively identified in the X-ray crystal

structures, a Zn_2 -coordinated water molecule in a similar position to Ser-102 of the wild-type enzyme is the proposed nucleophile in the S102G and S102A reactions [27]. Comparable phosphate binding modes and phosphate binding affinities (K_i) between the mutant enzymes and the wild-type enzyme suggest this is the case. The ability of the S102G and S102A enzymes to carry out catalysis in the absence of a nucleophilic residue or a covalent E-P intermediate illustrates the importance of the metal ions in creating the proper electrostatics and geometry for catalysis.

5.2. Arg-166 is primarily responsible for phosphate/substrate binding

Based on X-ray crystal structures, Arg-166 uses its guanidinium group to stabilize the transition state and to directly interact with the substrates/products of the reaction. Mutation of Arg-166 (R166Q, R166S, and R166A) [29,30] has very little effect on the activity (k_{cat}) in the presence of a phosphate acceptor, however, substrate binding decreases over 50-fold under the same conditions. Phosphate inhibition is also reduced 50-fold for the R166A and R166S mutant enzymes compared to the wild-type enzyme [30]. The removal of Arg-166 weakens both substrate and phosphate binding illustrating the important role of this residue in the initial binding of substrate and in the release of inorganic phosphate from the non-covalent complex. Since Arg-166 nor its positive charge is absolutely required for catalysis (i.e. k_{cat} is not significantly altered), however, these studies also emphasize the importance of the electropositive metal ions in attracting and stabilizing the negatively charged phosphate monoester/phosphate in the active site for hydrolysis.

5.3. Site-specific mutagenesis has been used to determine the functional significance of the Mg ion and residues not directly involved in catalysis

Three residues, Asp-101, Asp-153, and Lys-328, form secondary interactions to phosphate through either a water molecule or Arg-166 (Fig. 3). Disruption of this electrostatic interactions via site-specific mutagenesis results in enzymes with reduced phosphate affinity [31–37]. For the site-specific mutants D153G and D101S, weaker phosphate binding can be attributed to the increased flexibility of the Arg-166 side chain which is no longer constrained by hydrogen bonds to its Asp-153 and Asp-101 neighbors. Faster phosphate release in the D153G and D101S enzymes is responsible for the 5-fold and 35-fold higher activity (k_{cat}) of these enzyme, respectively. Smaller point mutations at Asp-101 do not alter phosphate binding, but still increase transphosphorylation activity suggesting that the increased mobility of Arg-166 increases the accessibility of the covalent E-P to phosphate acceptors [31]. Lower phosphate affinity for a series of mutations at Lys-328 (K328A, K328H, and K328C) does not reflect perturbations in the position of Arg-166. Instead, phosphate is shifted away from the active site pocket toward solvent due to the elimination of the water-mediated interaction with Lys-328. These studies illustrate the importance of secondary interactions in phosphate stabilization and further confirm this role for Arg-166.

Several active site mutations have been shown to alter the rate-limiting step in the mechanism. Among these are mutations made at Lys-328, Arg-166, and Asp-153 [34,37,38]. For these enzymes, the rate-limiting step changes from the release

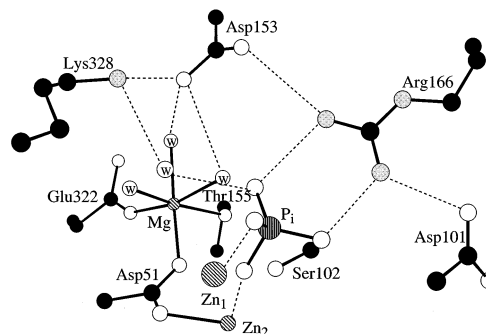


Fig. 3. Active site region of *E. coli* AP including bound phosphate, magnesium ion, and two zinc ions. Not all the metal ion ligands are shown for clarity. Water molecules are shown with an encircled letter w. Hydrogen bonds are shown as broken lines. This figure was drawn using coordinates from the Protein Data Bank file 1ALK.

of phosphate in the non-covalent E-P_i complex to the hydrolysis of the covalent E-P intermediate based on pre-steady-state kinetic studies and/or ^{32}P labeling experiments. The change in rate-limiting step for point mutants K328A, K328C, K328H, and R166A reflects the important role of Lys-328 and Arg-166 in lowering the pK_a of the Zn_1 -coordinated water molecule required for dephosphorylation of the covalent E-P intermediate. Replacing these positively charged residues with neutral ones (Ala and His) or a negatively charged one (Cys) results in reduced hydrolysis activity and enhanced transphosphorylation in the steady state [38]. The reduction in hydrolysis activity reflects the lower concentration of the Zn_1 -coordinated nucleophile while the enhanced transphosphorylation reflects the increased accessibility of E-P to phosphate acceptors. In contrast, the hydrolysis activity of the D153H mutant is about the same as the wild-type enzyme showing that this negatively charged residue does not participate in the generation of a Zn_1 -coordinated molecule. The change in rate-limiting step for this enzyme is probably due to the increased stability of the E-P complex [36]. Based on the structure of the D153H mutant, non-covalently bound phosphate adopts an orientation resembling the covalent E-P intermediate. In the absence of a salt link with Asp-153, Lys-328 can swing down and directly interact with phosphate altering its orientation and increasing its stability in the D153H enzyme. Based on these studies, the hydrogen bonding network and the electrostatic potential of the active site play an important role in controlling the rate-limiting step of the catalytic mechanism.

The importance of magnesium in increasing the activity of the zinc-containing enzyme has long been recognized [39,40], however, the specific roles of magnesium in catalysis and structural stabilization have been determined through site-specific mutagenesis of Asp-153 and Asp-51 [33,34,36]. The D153G, D153H, and D153H/K328A double mutant (DM) have reduced magnesium affinities. Maximal activity is only achieved with the addition of exogenous magnesium. Based on the X-ray structure [33], weaker magnesium affinity in the D153G enzyme is attributed to longer and presumably weaker interactions between this metal ion and its ligands. In the D153H enzyme and the DM [10,36], weaker magnesium binding is the result of converting the octahedral magnesium binding site to a distorted tetrahedral zinc binding site. From structural studies of D153H enzyme and the DM, the time-

dependent and reversible Mg activation of these enzymes can be interpreted as the slow replacement of zinc in the M3 site with magnesium. The magnesium occupation may reestablish the more open octahedral coordination sphere about the M3 metal ion thus restoring maximal activity. The octahedral geometry around magnesium in the M3 site appears to be important in holding the Asp-51 carboxylate side chain in an orientation to alternatively donate and withdraw electron density between Mg and Zn₂ during the course of the reaction [41]. Elimination of the functional link between Mg and Zn₂ in the D51N mutant enzyme results in the vacancy of the Mg site and a 20–40-fold less active enzyme. Based upon these studies, magnesium is required in the M3 site to structurally stabilize the enzyme in its catalytically most active form.

Asp-153 and Lys-328 are two of the three active site residues that differ between the *E. coli* enzyme and the mammalian alkaline phosphatases. These positions are occupied by histidine residues in the mammalian enzymes. The D153H single mutant and the D153H/K328H double mutant resulting from point mutations at positions 153 and 328 exhibit many properties of the mammalian enzymes including a more alkaline pH versus activity profile, decreased thermal stability, and magnesium activation [10,34,36]. Based on these studies, mutations at Asp-153 and Lys-328 appear to be responsible for many of the differences between the bacterial enzyme and the mammalian enzymes.

6. Concluding remarks

Alkaline phosphatase, a highly efficient enzyme catalyzing reactions close to the diffusion-controlled limit, utilizes a very simple active site architecture involving two zinc ions to carry out most of its rate acceleration. Site-specific mutagenesis of the nucleophile, Ser-102, supports this conclusion. Magnesium plays an indirect but important role in stabilizing the enzyme in its most active conformation. The hydrogen bonding network and the electrostatic field of the active site environment created by residues in the immediate vicinity influence phosphate stabilization and catalysis.

References

- [1] Reid, T.W. and Wilson, I.B. (1971) in: *The Enzymes*, Vol. 4 (Boyer, P.D., Ed.), pp. 373–415, Academic Press, New York.
- [2] Gettins, P. and Coleman, J.E. (1983) *J. Biol. Chem.* 258, 396–407.
- [3] Coleman, J.E., Nakamura, K. and Chlebowski, J.F. (1983) *J. Biol. Chem.* 258, 386–395.
- [4] Simopoulos, T.T. and Jencks, W.P. (1994) *Biochemistry* 33, 10375–10380.
- [5] Kaneko, Y., Hayashi, N., Toh-e, A., Banno, I. and Oshima, Y. (1987) *Gene* 58, 137–148.
- [6] Kam, W., Clauser, E., Kim, Y.S., Kan, Y.W. and Rutter, W.J. (1985) *Proc. Natl. Acad. Sci. USA* 82, 8715–8719.
- [7] Berger, J., Garattini, E., Hua, J.C. and Udenfriend, S. (1987) *Proc. Natl. Acad. Sci. USA* 84, 695–698.
- [8] Weiss, M.J., Henthorn, P.S., Lafferty, M.A., Slaughter, C., Raducha, M. and Harris, H. (1986) *Proc. Natl. Acad. Sci. USA* 83, 7182–7186.
- [9] Kim, E.E. and Wyckoff, H.W. (1989) *Clin. Chim. Acta* 186, 175–188.
- [10] Murphy, J.E., Tibbitts, T.T. and Kantrowitz, E.R. (1995) *J. Mol. Biol.* 253, 604–617.
- [11] Hough, E. et al. (1989) *Nature* 338, 357–360.
- [12] Volbeda, A., Lahm, A., Sakiyama, F. and Suck, D. (1991) *EMBO J.* 10, 1607–1618.
- [13] Wilson, I.B. and Dayan, J. (1965) *Biochemistry* 4, 645–649.
- [14] Schwartz, J.H. and Lipmann, F. (1961) *Proc. Natl. Acad. Sci. USA* 47, 1996–2005.
- [15] Wilson, I.B., Dayan, J. and Cyr, K. (1964) *J. Biol. Chem.* 239, 4182–4185.
- [16] Dayan, J. and Wilson, I.B. (1964) *Biochim. Biophys. Acta* 81, 620–623.
- [17] Jones, S.R., Kindman, L.A. and Knowles, J.R. (1978) *Nature* 275, 564–565.
- [18] Otvos, J.D., Alger, J.R., Coleman, J.E. and Armitage, I.M. (1979) *J. Biol. Chem.* 254, 1778–1780.
- [19] Gettins, P. and Coleman, J.E. (1983) *J. Biol. Chem.* 258, 408–416.
- [20] Gettins, P. and Coleman, J.E. (1984) *J. Biol. Chem.* 259, 4991–4997.
- [21] Gettins, P., Metzler, M. and Coleman, J.E. (1985) *J. Biol. Chem.* 260, 2875–2883.
- [22] Hull, W.E., Halford, S.E., Gutfreund, H. and Sykes, B.D. (1976) *Biochemistry* 15, 1547–1561.
- [23] Kim, E.E. and Wyckoff, H.W. (1991) *J. Mol. Biol.* 218, 449–464.
- [24] Murphy, J.E., Stec, B., Ma, L. and Kantrowitz, E.R. (1997) *Nature Struct. Biol.* 4, 618–622.
- [25] Holtz, K.M., Stec, B. and Kantrowitz, E.R. (1999) *J. Biol. Chem.* 274, 8351–8354.
- [26] Butler-Ransohoff, J.E., Rokita, S.E., Kendall, D.A., Banzon, J.A., Carano, K.S., Kaiser, E.T. and Matlin, A.R. (1992) *J. Org. Chem.* 57, 142–145.
- [27] Stec, B., Hehir, M.J., Brennan, C., Nolte, M. and Kantrowitz, E.R. (1998) *J. Mol. Biol.* 277, 647–662.
- [28] Han, R. and Coleman, J.E. (1995) *Biochemistry* 34, 4238–4245.
- [29] Butler-Ransohoff, J.E., Kendall, D.A. and Kaiser, E.T. (1988) *Proc. Natl. Acad. Sci. USA* 85, 4276–4278.
- [30] Chaidaroglou, A., Brezinski, D.J., Middleton, S.A. and Kantrowitz, E.R. (1988) *Biochemistry* 27, 8338–8343.
- [31] Chaidaroglou, A. and Kantrowitz, E.R. (1989) *Protein Eng.* 3, 127–132.
- [32] Chen, L., Neidhart, D., Kohlbrenner, W.M., Mandecki, W., Bell, S., Sowadski, J. and Abad-Zapatero, C. (1992) *Protein Eng.* 5, 605–610.
- [33] Dealwis, C.G., Chen, L., Brennan, C., Mandecki, W. and Abad-Zapatero, C. (1995) *Protein Eng.* 8, 865–871.
- [34] Janeway, C.M., Xu, X., Murphy, J.E., Chaidaroglou, A. and Kantrowitz, E.R. (1993) *Biochemistry* 32, 1601–1609.
- [35] Mandecki, W., Shallcross, M.A., Sowadski, J. and Tomazic-Alen, S. (1991) *Protein Eng.* 4, 801–804.
- [36] Murphy, J.E., Xu, X. and Kantrowitz, E.R. (1993) *J. Biol. Chem.* 268, 21497–21500.
- [37] Xu, X. and Kantrowitz, E.R. (1991) *Biochemistry* 30, 7789–7796.
- [38] Sun, L., Martin, D.C. and Kantrowitz, E.R. (1999) *Biochemistry* 38, 2842–2848.
- [39] Bosron, W.F., Anderson, R.A., Falk, M.C., Kennedy, F.S. and Vallee, B.L. (1977) *Biochemistry* 16, 610–614.
- [40] Anderson, R.A., Bosron, W.F., Kennedy, F.S. and Vallee, B.L. (1975) *Proc. Natl. Acad. Sci. USA* 72, 2989–2993.
- [41] Tibbitts, T.T., Murphy, J.E. and Kantrowitz, E.R. (1996) *J. Mol. Biol.* 257, 700–715.
- [42] Evans, S.V. (1993) *J. Mol. Graph.* 11, 134–138.